JGR Oceans

RESEARCH ARTICLE
10.1029/2020JC017093

A Shift in the Wind Regime of the Southern End of the Canary Upwelling System at the Turn of the 20th Century

D. Gallego[1], R. García-Herrera[2,3], T. Losada[2], E. Mohino[2], and B. Rodríguez de Fonseca[2,3]

[1]Departamento de Sistemas Físicos, Químicos y Naturales, Universidad Pablo de Olavide, Seville, Spain, [2]Departamento de Física de la Tierra y Astrofísica, Universidad Complutense, Madrid, Spain, [3]IGEO, Instituto de Geociencias (CSIC, UCM), Madrid, Spain

Key Points:

- Historical wind observations can be used to calculate the upwelling intensity at the Senegal-Mauritanian coasts since the mid-19th century
- Winds over the Senegal-Mauritania coast may have experienced a shift around the year 1900

Correspondence to:
D. Gallego,
dgalpuy@upo.es

Citation:
Gallego, D., García-Herrera, R., Losada, T., Mohino, E., & Rodríguez de Fonseca, B. (2021). A shift in the wind regime of the southern end of the Canary upwelling system at the turn of the 20th century. *Journal of Geophysical Research: Oceans*, *126*, e2020JC017093. https://doi.org/10.1029/2020JC017093

Received 17 DEC 2020
Accepted 4 MAY 2021

Abstract In this study, we make use of historical wind direction observations to assemble an instrumental upwelling index (DUI) at the southern end of the Canary Current Upwelling System. The DUI covers the period between 1825 and 2014 and, unlike other upwelling indices, it does not rely neither in wind speed nor in reanalyzed data. In this sense, the DUI can be regarded as an instrumental index. Additionally, it avoids the suspected bias toward increasing wind speed of historical wind observations documented in previous research. Our results indicate that the frequency of the alongshore winds at the west coast of Africa between 10°N and 20°N measured by the DUI is significantly related with the wind stress and therefore the upwelling intensity in this region. The DUI presents a significant variability both at interannual and decadal timescales. We have not found any significant trend for the 20th century. However, when the entire length of the series is considered, a large shift toward more frequent alongshore winds is evidenced as a result of several decade-long fluctuations which took place between the late 19th century and the beginning of the 20th century. This fact would imply that a significant change in the upwelling intensity at the southern end of the Canary Current Upwelling System should have occurred at the turn of the 20th century.

Plain Language Summary Along the coasts of Northwestern Africa, friction of the predominant winds results in an upward motion of sea water from intermediate depths toward the ocean surface. This phenomenon is known as "coastal upwelling" and it has a huge economic and social relevance. Cold upwelled water is rich in nutrients and yields very productive marine ecosystems. Therefore, knowing the changes of the upwelling intensity is of great importance. Unfortunately, prior to the 1950s, the scarcity of wind observations along these coasts difficulties the estimation of the coastal upwelling intensity, making the climatic history of this system uncertain. Since the late 18th century, a lot of ships have circumnavigated the African continent. Most of them took observations of wind direction that have come to the present day in form of records preserved in the ships' logbooks. In this study, we make use of these historical observations to calculate the intensity of the coastal upwelling. We have found that coastal upwelling in Northwest Africa is highly variable at decadal scale and we provide a strong evidence of a large change in the upwelling intensity that occurred around 1900.

1. Introduction

Four major Eastern Boundary Upwelling Systems exist in the global Ocean. Among them, the Canary Current Upwelling System (CCUS) extends from the coast of West Africa, approximately at 10°N, to the coast of Galicia in northern Spain, around 45°N (Aristegui et al., 2009). The upwelling characteristics along the CCUS are strongly dependent on the latitude (Benazzouz et al., 2014). Its southern edge comprises the coasts of Mauritania, Senegal, Gambia, and Guinea. Along these coasts upwelling is distinctly seasonal, and highly dependent on the latitudinal migration of the Intertropical Convergence Zone (ITCZ). At these latitudes, the upwelling season comprises from January to May, when persistent equatorward winds blow along the NW African coast inducing an Ekman transport perpendicular to the wind stress. As the ITCZ migrates to the north from late spring into the summer, south-westerly winds associated with the West African Summer Monsoon dominate in this area (Gallego, Ordóñez, et al., 2015) inhibiting upwelling.

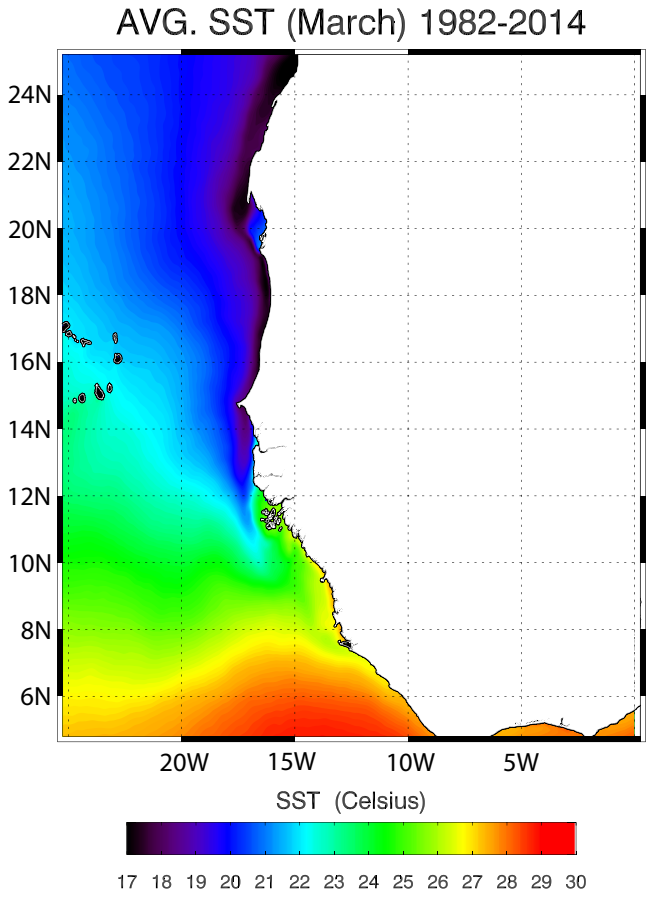

Figure 1. Average March SST based on daily Operational Sea Surface Temperature and Sea Ice Analysis (OSTIA) SST data (Good et al., 2020) from 1982 to 2014.

It must be stressed that two sectors can be distinguished within the 10°N–20°N latitude band. Between 14°N and 20°N the shelf is relatively narrow, and the Ekman transport driven by the alongshore trade winds is the main modulator of the upwelling intensity (Cropper et al., 2014; Sylla et al., 2019). Upwelling is there seen as a relatively narrow band of SST minima next to the coast in the monthly averages (Figure 1). South of 14°N the continental shelf is broad and shallow. There, the wind stress can be largely balanced by bottom friction (Ndoye et al., 2014). This reduces the relative importance of the Ekman transport and increases the contribution of the Ekman pumping driven by cyclonic wind stress curl (Jacox & Edwards, 2012). The progressive relevance of this curl-driven upwelling southward of the 14°N latitude is evidenced by the broader extension of the SST minima and the location of the cold tongue, which is found further away from the shore. Comparatively to other upwelling areas, and despite the high levels of primary production characteristic of this region, the southern end of the CCUS has so far received little attention (Ndoye et al., 2014), especially from the long (decadal) term perspective. This is in part due to the scarcity of climatological series adequate to quantify upwelling intensity.

Historically, upwelling intensity has been quantified either by using SST-based indices or through dynamical indices based on the alongshore wind strength. SST derived indices are typically defined as the difference between SST near the coast and those in the open ocean (Narayan et al., 2010). However, the cold SST surge can be restricted to a few tens of km from the coast or even less, and it usually involves SST differences in the order of 2°C to 3°C. Thus, the generation of reliable SST indices requires high-resolution fields that at the southern edge of the CCUS are only attainable by using satellite retrievals and complex definitions of the meaning of "open ocean" (Benazzouz et al., 2014). These facts severely limit the length of any upwelling series based on SSTs. Most importantly, SST-based indices have caveats, as the changes in the longitudinal SST gradient cannot always be directly attributed to coastal upwelling (Cropper et al., 2014). External factors such as the freshwater input from river's discharge, the effect of synoptic-scale weather systems or the heterogeneity of the depth of the oceanic mixed-layer strongly interfere the SST signal, limiting the ability of these indices to unambiguously characterize the upwelling intensity.

In order to cope with these difficulties, wind-derived indices have been preferably used in the literature to analyze the long-term variability of upwelling systems (Barton et al., 2013; Gomez-Gesteira et al., 2008; Santos et al., 2012; Sylla et al., 2019). A large part of these indices just uses the zonal component of the Ekman mass transport, which is directly proportional to the meridional component of the wind-stress. Other indices calculate the rotational of the wind stress which is the convergence of the total Ekman mass transport and, from the continuity equation, indicates the total water upwelled. Nevertheless, it has been demonstrated that the former definition is good enough and simplifies the problem (Sylla et al., 2019).

Wind-based indices are also affected by difficulties. Almost every attempt to build a long-term dynamical upwelling index has made use of the ICOADS (International Comprehensive Ocean-Atmosphere Data Set) (Freeman, Woodruff, et al., 2016) wind observations and/or reanalysis products such as the NCEP/NCAR reanalysis (Kalnay et al., 1996) or the ERA-40 reanalysis (Uppala et al., 2005), both strongly relying on assimilated ICOADS observations (Wohland et al., 2019) thus inheriting some of the ICOADS characteristics. This constitutes a serious problem when analyzing long-term trends of wind derived magnitudes. ICOADS has proven to be an invaluable source of data for climatic analysis since decades ago (Cardone et al., 1990; Ramage, 1987), but it is suspected that ICOADS wind velocities are biased toward increasing values, resulting in unrealistic positive trends for the wind speed (Barton et al., 2013). This problem has been attributed

to the gradual shift from visually estimated to anemometer-measured winds, an increase in anemometer height and ship's size (Thomas et al., 2008), discrepancies in the interpretation of the Beaufort scale by mariners of different tradition (Barton et al., 2013; Gallego, Garcia-Herrera, et al., 2007) and changes in the relative frequencies of measured and estimated winds (Bakun et al., 2010). Although these observer-induced trends are relatively small, they can be decisive for some applications, such as the estimation of subtle trends in a variable—the alongshore wind stress—, which is proportional to the square of the wind speed magnitude. The biases in ICOADS are especially relevant prior to the 1940s (Thomas et al., 2008) and, probably as a result of this, to the best of our knowledge, there have been no published attempts to use neither pure ICOADS nor ICOADS-derived products (i.e., 20th century reanalysis) to build century long upwelling indices (Sydeman et al., 2014).

The problems arising from the use of wind speed measurements in historical times have recently led to a different approach based on the generation of climatic indices relying on the wind direction alone, the so-called "directional indices." This approach implicitly assumes that the persistence of winds in a given direction is significantly correlated with the magnitude of the wind in the monthly averages. Directional indices can be considered instrumental ones, as even the oldest observations of wind direction do not need subjective judgments or re-scaling to modern standards beyond the conversion from magnetic to geographic coordinates (Jackson et al., 2000; Jones & Salmon, 2005; Wheeler et al., 2009). This methodology has allowed for the generation of the longest series of the wind circulation that can be considered purely instrumental in the North Atlantic (Barriopedro et al., 2014; Mellado-Cano, Barriopedro, García-Herrera, & Trigo, 2020) and it has proven to be very sensitive to fine details of the wind circulation as well. For instance, directional indices have permitted the determination of the influence of large volcanic eruptions on the strength of the West African Summer monsoon during the 19th century (Gallego, Ordóñez, et al., 2015), the determination of the Indian Summer Monsoon onset (Ordoñez et al., 2016), the finding of a secular trend in the strength of the Australian Summer Monsoon (Gallego, García-Herrera, et al., 2017) or quantifying the jet variability over the Atlantic (Mellado-Cano, Barriopedro, García-Herrera, Trigo, et al., 2019), among other examples of multidecadal variability (Garcia-Herrera et al., 2018).

Upwelling at the southern edge of the CCUS is an excellent candidate to be studied by means of directional indices, because in a first approximation the problem can be addressed by analyzing the stationarity of northerly winds. Moreover, this is a region rich in historical wind observations over the ocean as, since the late 18th century, a lot of ships circumnavigated the Northwestern coast of Africa. Most of them took daily observations of wind direction that have come to the present day in form of written records preserved in the ships' logbooks. Due to the uniqueness and interest of these early observations, a number of international projects such as CLIWOC (García-Herrera et al., 2005), ACRE (Allan et al., 2011), or RECLAIM (Wilkinson et al., 2011) among many others have been devoted to unveil these valuable data which are nowadays incorporated in the ICOADS database (Woodruff et al., 2010). Furthermore, it has been estimated that thousands of wind observations in this area, potentially useful for characterizing the winds at the CCUS southern tip, are still not included in ICOADS (Wheeler & García-Herrera, 2008).

The aim of this study is to evaluate the variability of the coastal upwelling at the southernmost tip of the CCUS since the early 20th century by developing a directional index based on these historical observations.

2. Methods

2.1. Data

To characterize the upwelling at the southern end of the CCUS we defined the box (10°N–20°N; 30°W–15°W) (SeM area from now on). Within this box (Figure 2), we considered wind direction observations from the following two sources:

1. Our main source of wind direction data was ICOADS in its 3.0 release. At the time of writing, this database contains over 455 million individual marine reports starting in 1662 and lasting up to 2014 (Freeman, Woodruff, et al., 2016). We used the raw (i.e., not gridded nor reanalyzed) wind direction observations. Shading in Figure 2b represents the density of raw ICOADS observations of wind direction along the NW African coasts, which shows a maximum density along the routes circumnavigating Africa and

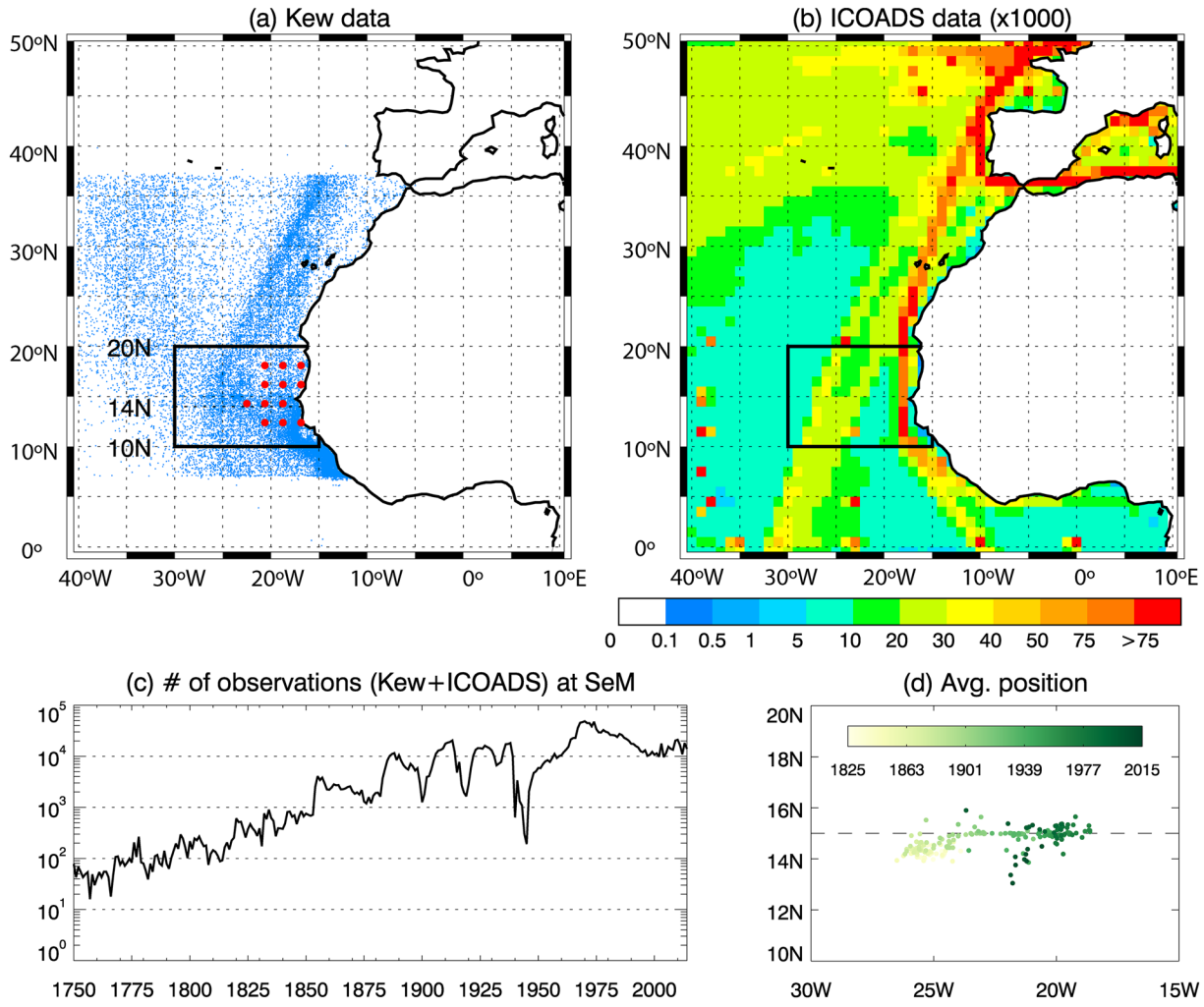

Figure 2. (a) Area selected to define the Directional Upwelling Index (DUI) for the Senegal-Mauritania (SeM) upwelling system. Blue dots represent individual wind direction observations taken from the Kew Archives for this research and red dots indicate the grid-points used for calibration based on NCEP-NCAR reanalysis 2 momentum flux. (b) ICOADS coverage in a 1°×°1 grid. (c) Evolution of the total (Kew + ICOADS) number of observations inside the SeM area used to compute the DUI. (d) Average latitude and longitude of the wind direction observations along the period 1825–2014 within the SeM area.

a secondary maximum related to the routes connecting Europe with South America. These predominant routes are well inside the selected SeM box.

2. As part of the "UPNAO" project aimed to improve the coverage of historical meteorological observations along the Northwestern African coast (see Acknowledgments), we undertook a systematic search of undigitized data in the UK National Archives at Kew (Surrey) concentrating on ships traveling from the UK mainland to Africa ("Cape, West Africa & St. Helena" series, AMD 51 and AMD 52). We digitized and abstracted a total of 67,339 new records of wind direction roughly covering the latitudes between 5°N and 45°N. The earliest and latest data correspond to 1776 and 1904, respectively. Small blue dots in Figure 2a represent the individual observations specifically abstracted for this research. As in the previous case, the maximum density of observations appears relatively close to the coast within the selected box and follows the predominant routes of the British ships toward Southern Africa.

Figure 2c shows the evolution of the annual combined (Kew + ICOADS) number of wind direction observations from 1750 to 2014 inside the SeM box. Up to 1850, the number of observations is below 1,000 per year and along the 1880s the number of observations ranges between 5,000 and 11,000 observations per year, with significant drops in data availability during the WW1 and especially, the years during and immediately after WW2. The temporal evolution of the average geographical location of the observations inside the SeM

box is displayed in Figure 2d. Despite the changes in the routes along the decades, the average latitude of the observations remained remarkably constant in time, being constrained between 14°N and 16°N, in the center of the sampling area. The longitude shows larger variability, reflecting the more frequent use of the routes from Europe to South America in earlier periods in relation with the routes aimed toward Central and South Africa, increasingly frequent since the mid-20th century.

It has been estimated that to compute a meaningful directional index an absolute minimum of 10 observations per month in different days is required. This corresponds to a minimum of 120 observations per year, although it is desirable having at least, 100 per month (Gallego, Ordóñez, et al., 2015). From Figure 2c it seems reasonable to compute a directional wind index at the SeM box starting at the 1820s decade, when the number of available annual observations first regularly exceeds the 120 observations per year mark at the SeM box. However, it must be noted that the desirable coverage of 100 observations per month is only attained from the 1850s decade on, when the number of observations clearly exceeds the 1,200 mark per year (Figure 2c).

Apart of raw wind direction observations, along this study, we make use of the following databases: NCEP/NCAR reanalysis 2 (Kanamitsu et al., 2002), 20CR reanalysis (Compo et al., 2011), ERA-20C reanalysis (Poli et al., 2016), and the most recent version of the daily Operational Sea Surface Temperature and Sea Ice Analysis (OSTIA) SST data from 1982 to 2014 at a resolution of 1/20° or ∼5 km (Good et al., 2020).

2.2. Index Definition

As our objective is the generation of a directional index directly related to the persistence of the alongshore winds from 20°N to 10°N we defined the so-called Directional Upwelling Index (DUI) as the relative number of days in a month with wind flowing from the north within the SeM area. The DUI is expressed as a percentage:

$$\mathrm{DUI}(\%) = 100 \cdot \frac{\text{number of days in a month with wind flowing from the North at SeM}}{\text{number of days in a month}}$$

Defining the precise meaning of "wind flowing from the North" by using a distribution of individual wind observations randomly spread over an area implies a calibration procedure. In this research a day has been considered "a day with prevalent wind flowing from the North" when a minimum percentage "MP" of the total number of available observations inside the SeM area indicates wind between 315° and 45° (±45° from the true North). The value of MP is initially unknown, and it has been derived from a calibration process aimed to optimize the correlation between the DUI and a calibrator (Garcia-Herrera et al., 2018). As a calibrator, we used the northward component of the NCEP/NCAR reanalysis 2 momentum flux averaged over the three grid points closest to the coast and inside the SeM area (red dots in Figure 2a). For calibration we took the 1982–2014 period. Although the NCEP/NCAR reanalysis 2 is available since 1979, we selected the 1982–2014 range for calibration to coincide with the period where the OSTIA SST data are available.

To determine the optimal value for MP we computed 71 different DUIs with MP ranging from 20% to 90% and then correlated these series with the NCEP/NCAR momentum flux. The maximum average correlation for the months between January and May (when upwelling in the SeM area is maximum) was found for MP = 65% (average correlation between the DUI and the momentum flux of $r = 0.48$). So, in the DUI definition, the numerator is the number of days in a month inside the SeM area in which more than 65% of the daily number of available observations indicate wind directions between 315° and 45°.

Figure 3 shows the seasonal evolution of the momentum flux used as a calibrator (blue dashed line) and the evolution of the calibrated DUI (black line). The correlations for each month between the calibrator and the DUI for the calibration period 1982–2014 are also shown. The seasonal evolution of the alongshore momentum flux is well captured by the DUI. Minimum values of the DUI are found in August (DUI = 15.1%) and September (DUI = 18.7%), the same months when the northward momentum flux is minimum inside the SeM box (0.018 $N \cdot m^{-2}$ in August and 0.025 $N \cdot m^{-2}$ in September). On the other hand, both DUI and northward momentum flux values are high from January to May with both variables reaching its maximum value in April (92.4% and 0.082 $N \cdot m^{-2}$ respectively). Correlations are significant during the core of the

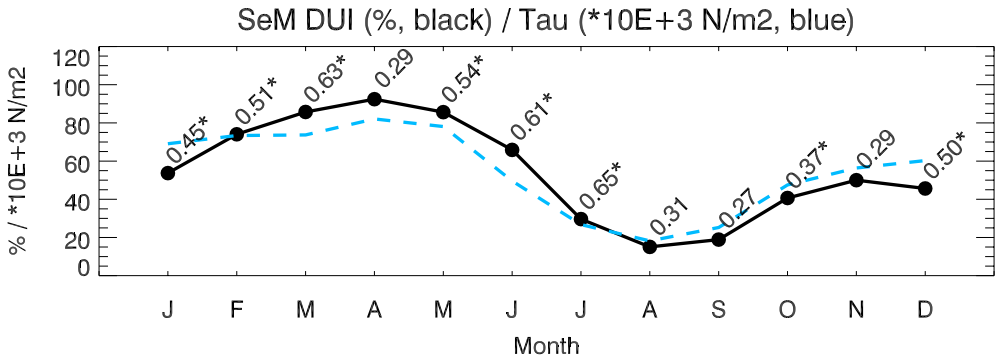

Figure 3. Monthly values of the NCEP/NCAR reanalysis 2 momentum flux (in·10^3 N·m^{-2}) averaged over the three grid points closer to the coast within the SeM box (blue dashed line). The corresponding DUI values (in %) are displayed by a black line. Numbers indicate the correlation between both series for the calibration period 1982–2014. Asterisks mark values statistically significant at the $p < 0.05$ level.

upwelling season except for the April case. Maximum correlation is found in March ($r = +0.63$, $p < 0.05$), the central month of the upwelling season.

2.3. Estimation of the DUI's Uncertainty

Computing a directional index by using historical wind direction measurements requires the acceptance of a compromise. On the one hand, the use of a relatively small region is desirable to minimize the spatial variability of the wind within the region. On the other hand, because of the low density of observations in historical times, large areas are necessary to have a reasonable number of observations. In our case, the SeM region covers an area over 1,500,000 km^2. The inherent spatial variability of the wind inside this region and the finite number of available measurements in each month are necessarily translated as uncertainty in a particular realization of the index based on a finite sample of observations. For a given month, a different set of observations taken at different places would lead to a different value of the DUI. As the number of available observations increases, the sampling will be more representative of the value of the wind direction persistence. In consequence, it is expected that the lower the number of available observations, the larger the uncertainty. To estimate the expected uncertainty of the DUI as a function of the number of available observations, we adopted a bootstrap approach as in Gallego, Ordóñez, et al. (2015). For every year and month between 1971 and 2010, 1000 "degraded" DUIs were constructed from "N" randomly selected wind observations inside the SeM area, with N ranging from 10 to 500. For each N, the 1000 degraded DUIs are different because they are computed from a different subset of the total available observations. The average standard deviation of these 1,000 series as a function of N for the months between January and May is shown in Figure 4. The results show that the uncertainty slightly depends on the month, but, in general, the largest standard deviations are found for $N = 10$ (around 13%–17%) in all cases, as expected. This value rapidly decreases as N increases. For $N = 50$ observations, the standard deviation ranges between 7% and 9%. And for $N = 500$ the expected deviation goes from 6% to 8% The fact that the standard deviation does not tend to zero as N increases reflects the inherent spatial variability of the wind inside the regions considered. We took the standard deviations displayed in Figure 4 as a conservative dispersion measure for a DUI computed from N observations. It must be pointed out that this dispersion measure is purely empirical, depends on the region and it should be only

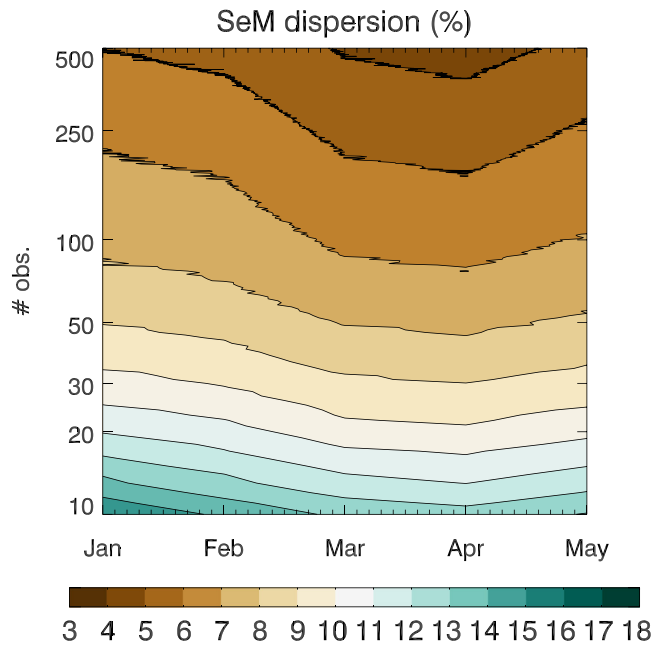

Figure 4. Expected dispersion (in %) of the DUI for the SeM box as a function of the number of wind direction observations used to compute it (*y*-axis) and for the months when each index is defined (*x*-axis).

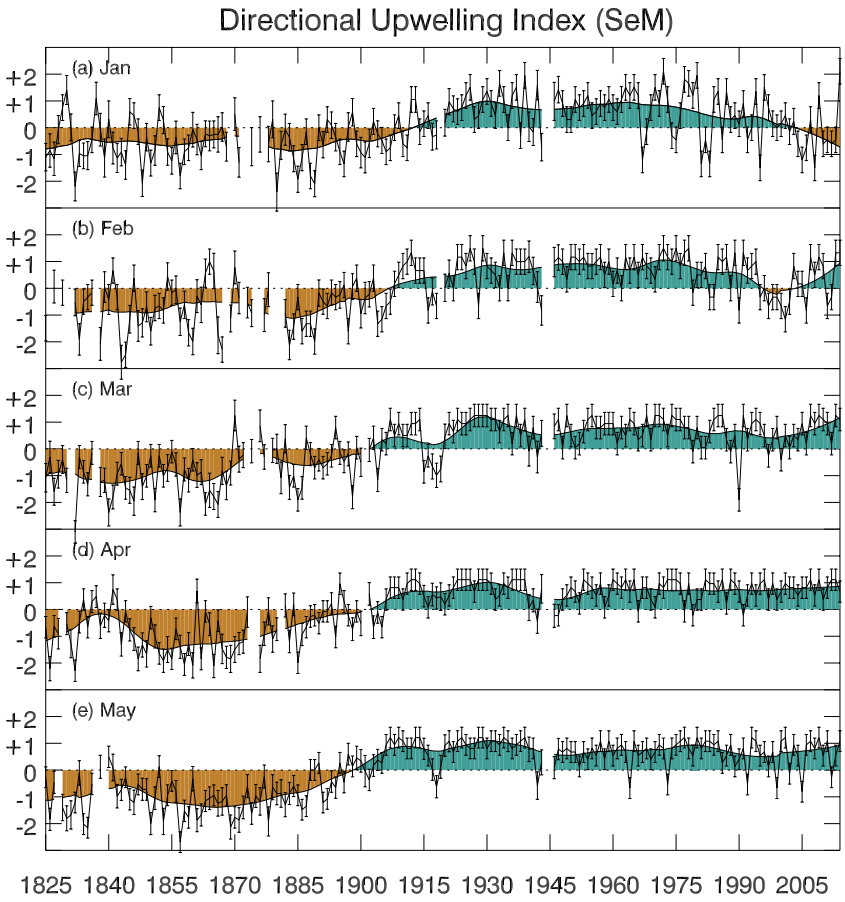

Figure 5. Standardized DUI for the SeM area from January to May between 1825 and 2014. Error bars indicate the expected standard deviation based on the number of observations available each year. Shaded curve is computed as a robust locally weighted regression with a 31-years window (Cleveland, 1979).

interpreted as the expected standard deviation of a DUI value computed from a particular set of wind direction measurements and not as a confidence interval in a statistical sense.

3. Results

3.1. The DUI Series

Figure 5 shows the standardized monthly DUI from January to May. In general, the DUI is highly variable at the sub-decadal scale, with noticeable short-term fluctuations of greater amplitude in January, at the beginning of the upwelling season. During this month, consecutive extreme values of opposite sign are commonly found, as for example at the beginning of the 1980s decade, with a standardized value of the DUI in 1980 of +1.95 (29 out of the 31 days of that January had prevalent northerly winds) followed by 3 years with a very low DUI of −1.35, −0.45, and −1.35 (7, 13, and 7 days displaying northerly winds respectively). Similar examples can be found along the entire January series. These short-term fluctuations are also found in February, as for example at the end of the series, but in general they are less frequent and of lower amplitude indicating that as the upwelling season progresses, the northerly winds at the SeM are more stable and less variable at the sub-decadal scale. Notwithstanding, extreme isolated values of the DUI can be found even during March, being the best example the case of 1990 with a standardized DUI of −1.97. On that March only 10 days out of 31 had prevalent northerly winds at SeM. It is interesting to note that except for January, the short-term variability is noticeably greater prior to 1900 than after this year. This is especially evident for April and May.

Superimposed to the short-term variability, longer term fluctuations are also evident, as reveals a locally weighted scatterplot smoothing (Haywood et al., 2013) performed with a 31-years window width (shaded curves in Figure 5). This method provides a robust estimation of the long-term changes of a time series with missing values (Cleveland, 1979). This analysis reveals a progressive change in the mean of the DUI for all months from negative to positive values. The change from predominantly negative to positive anomalies occurs around 1900 in all cases. In this sense, a linear trend analysis performed over sliding windows of variable width (Figure 6) shows that in general the shift from negative to positive DUI anomalies did not occur in a single step but as the result of a sequence of several decade-long fluctuations which took place along the late 20th century and the first two decades of the 20th century. This is demonstrated by the alternating sign of the linear trends around 1900 when they are computed over short windows (15–25 years, see Figure 6c for example). When the linear trends are computed over wider windows (40–50 years), it is evidenced that in general, the shift in the values of the DUI occurred between 1870 and 1920, being the long-term trend positive and statistically significant ($p < 0.05$) in this period.

3.2. Relation of the DUI With SST Anomalies

The calibration procedure summarized in Figure 3, demonstrates that the DUI based on the persistence of northerly wind direction is significantly correlated with the alongshore wind stress in the coast of Senegal. In this section, we explore the changes in the SST related to the DUI variability. For this purpose, we use the monthly averages of the daily Operational Sea Surface Temperature and Sea Ice Analysis (OSTIA) SST (Good et al., 2020). For each month within the upwelling season, we computed the difference between the monthly average SST for the years when the DUI is over the 90% percentile minus the years with DUI below the 10% percentile over the common period 1982–2014 covered both by the OSTIA SST data set and our DUI.

Figure 7 shows that although the typical geographical distribution of the anomalies does not reveal the pattern associated with a pure Ekman transport, the years with high DUI consistently show lower SSTs. During January (Figure 7a) and March (Figure 7c) the SSTs along the coast can be up to 2.0°C lower for the cases with large DUI. The longitudinal extension of the SSTs anomaly associated with positive DUI extremes is clearly noticeable in these months (Capet et al., 2017), although during January, Figure 7 does not show a low SST band next to the coast northward of 16°N as it would be expected. Evidence of an enhanced upwelling for large DUIs is also evident for February, April and May (Figures 7b–7d and 7respectively), although in these cases, the SST changes are not as intense, but they are mostly constrained to the coastal area as expected from changes in the alongshore winds represented by the DUI.

The high resolution of the OSTIA data set, allows the assessment of specific cases of high and low DUI values beyond the averages shown in Figure 7. Figure 8a shows the difference in SST for February 2014, a month characterized by a large DUI (DUI = +1.33 in standardized units) minus the SST in February 2001, with the lowest in the series (DUI = −1.16). Figure 8b shows the case of March 1991 a year with a large DUI = +1.25 which was preceded by the year 1990, which displayed the lowest DUI of the series within the 1982–2014 period for March (DUI = −1.91). In both cases, the colder SST associated with large DUIs are quite evident, although this analysis also indicates that southward of 12°N, the SST anomaly immediately next to the coast is small, suggesting that the DUI is not a good measure of the local coastal upwelling in this area.

3.3. Comparison With Reanalysis Data

ICOADS is a fundamental source of data of historical reanalysis. The 20CR reanalysis assimilates ICOADS surface and sea-level pressure, whereas ERA-20C additionally assimilates ICOADS surface winds. In this sense, a direct comparison between the DUI and any variable on these datasets is necessarily incestuous, and this especially applies for near surface reanalyzed winds. Notwithstanding, we consider this comparison interesting because the DUI is free of some of the biases that affect reanalyzes and, these biases represent a key impediment at the time of computing long-term trends.

In reanalyzes, data assimilation techniques are used in combination with global forecast models to produce data fields based on multiple observational sources, this is known as the “observational constrain”

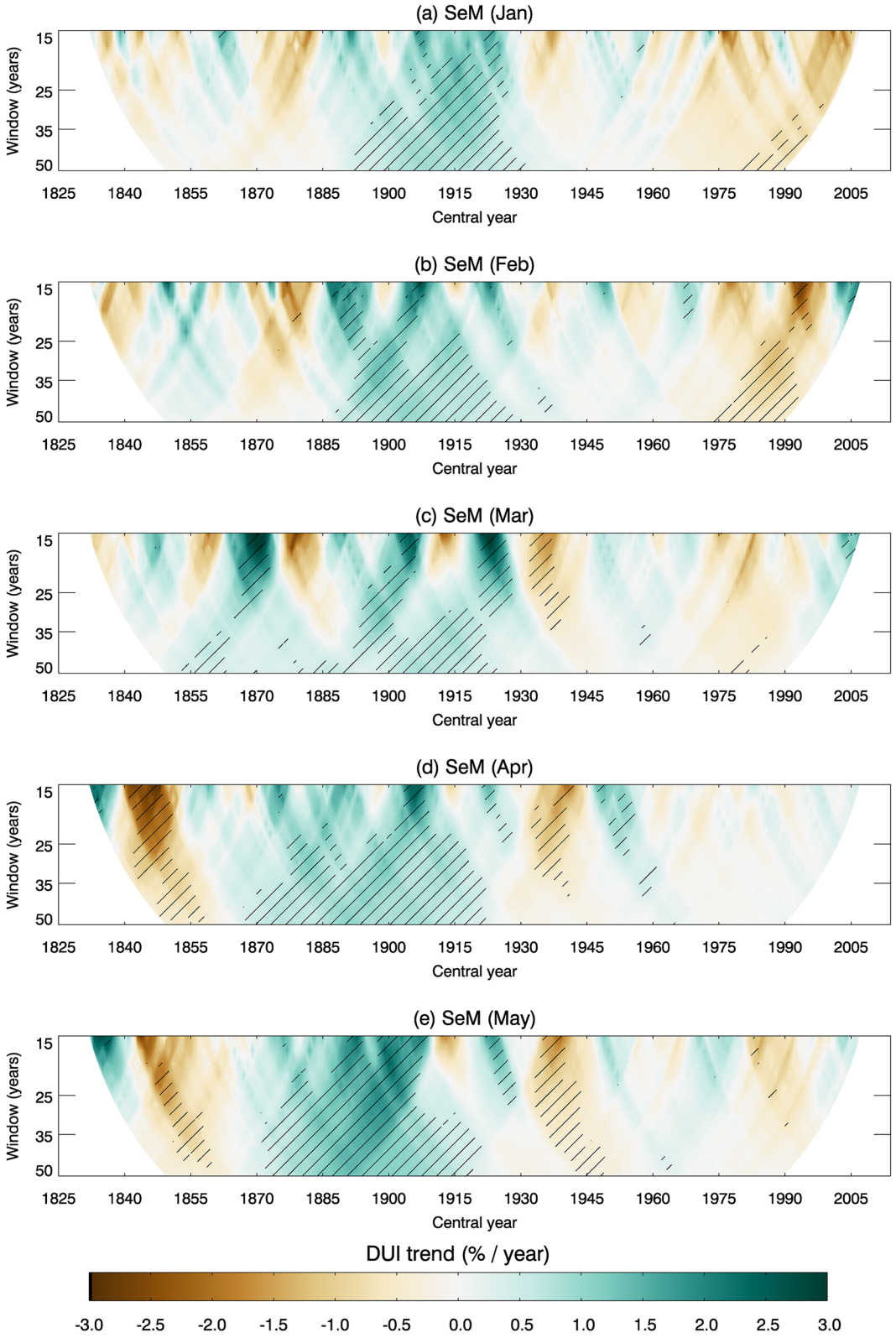

Figure 6. Linear trends of the DUI for the SeM area (in % per year) for a sliding window centered at the year indicated on the *x*-axis and width indicated on the *y*-axis. Hatched areas indicate statistically significant trends at $p < 0.05$. *x*-axis is escalated as in Figure 5 to ease comparison.

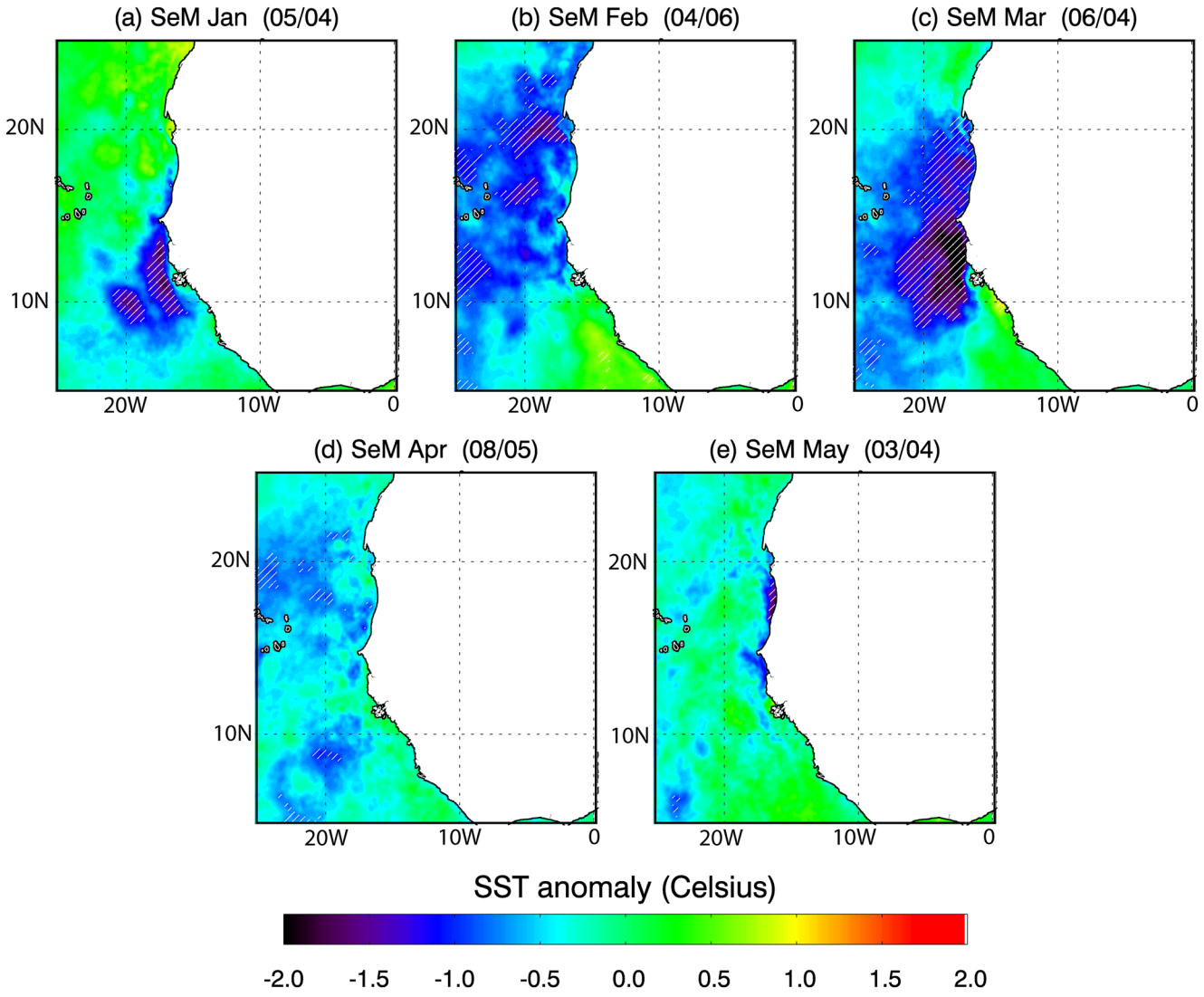

Figure 7. Difference between the monthly average SST data from the Operational Sea Surface Temperature and Sea Ice Analysis for the years in which the DUI computed at the SeM box is over the 90% percentile minus the years with DUI below the 10% percentile over the period 1982–2014. Numbers over each case indicate the number of cases over the 90% percentile/below the 10% percentile included in each composite. Hatched areas indicate significant differences based on a 1,000 trial bootstrap procedure.

(Bosilovich et al., 2013). The main advantages of this approach are that reanalysis data are available at all points in space and time and that the produced fields are physically consistent. However, it is widely recognized that the confidence that can be placed in reanalyzed fields is strongly dependent upon the number and quality of the observations that conform the observational constrain (Brönnimann et al., 2018; Compo et al., 2011; Hersbach et al., 2017; Uppala et al., 2005). In the case of historical reanalysis, the number and nature of the observations have changed considerably from the 19th century to the present time (Slivinski, 2018). This, along with the presence of biases associated with observations and models, such as the one documented for the wind speed on ICOADS (Barton et al., 2013), could introduce spurious trends into reanalysis-derived indices.

Our DUI is also affected by the changes in data coverage, but as it is solely computed from the raw wind direction, it is free of the problem associated with the wind speed. Additionally, the DUI can be regarded as an instrumental index (García-Herrera et al., 2018) and therefore it is not affected by any possible model-induced bias. In this context, we consider interesting to compare the variability of our instrumental DUI with analogous indices built from historical reanalysis.

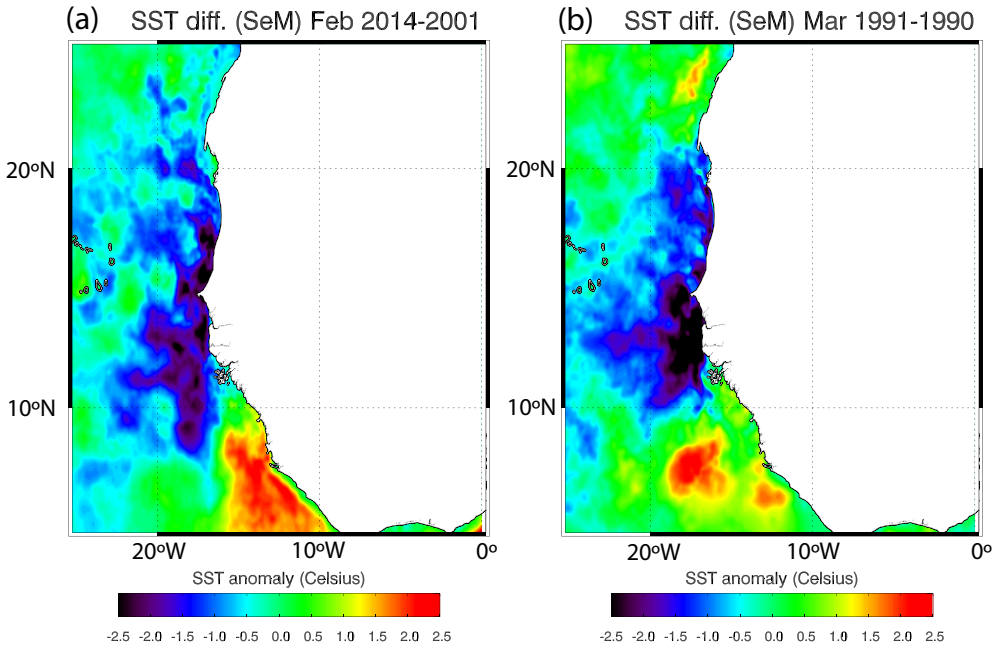

Figure 8. Difference between OSTIA based SST averaged for (a) February 2014 (DUI = −1.33) and 2001 (DUI = −1.16) and (b) March 1991 (DUI = +1.25) and 1990 (DUI = −1.91). All DUI values are given in standardized units.

We computed the near surface wind vector spatially averaged over the grid points inside the SeM box from the 20CR (0.995-sigma level) and the ERA-20C reanalysis (10m level). As in our original definition for the DUI, we calculated the monthly percentage of days inside this region in which this average wind indicates wind flowing between ± 45° from the true North for the periods 1851–2014 (20CR) and 1900–2010 (ERA-20C). To compare the series, we performed a sliding correlation using a 31-years window between our original DUI based on direct wind direction observations (ICOADS) and the DUI based on reanalysis.

Figures 9a and 9b show two representative cases corresponding to January and March. We have selected these two cases because they constitute good examples of the differences between the observed and the reanalyzed versions of the DUI at the beginning and the core of the upwelling season. Figure 9b shows that the reanalysis versions of the DUI are frequently "locked" to their maximum value in March. This is especially noticeable for the 20CR version (red line in Figure 9b) and years of low data coverage (before the 1950s decade). This strongly suggest that during the core of the upwelling season and on years of poorer data coverage, the reanalysis displays lower variability than our DUI. This is not observed in January (Figure 9a), at the beginning of the upwelling season when the wind is more variable in direction both in the reanalyzed data and on the ICOADS observations. Otherwise of this detail, the observed DUI and the reanalyzed versions are quite similar for most of the second half of the 20th century. During this period, the sliding correlations are high, and they are consistently significant ($p < 0.05$) for January (Figure 9c) for both reanalyzes. With lower correlation values, this behavior is also observed for March (Figure 9d), although in this case, the 20CR index displays higher correlations. Interestingly, for years prior to the 1950s decade, the correlations between the DUI and their reanalyzed counterparts dramatically drop toward nonsignificant values. In January, with some exceptions such as a few years around 1920 and the late 1870s, the correlations drop to values close to zero. In March, the correlations remain positive and around +0.3 up to the 1930s, but for the previous period correlations are close to zero, with the exception of the period spanning from 1885 to 1914, when the correlation between the original DUI and the DUI based in 20CR is negative, reaching statistical significant values during the first 10 years of the 20th century.

It is interesting to point out that Figure 9 also shows noticeable discrepancies between both reanalysis prior to the 1930s decade. In this sense, in a recent study Vega et al. (2017) found that even although the observational constraint of 20CR and ERA20C is strongly linked, as they share a significant part of the observational input, wind circulation indices computed from these datasets can disagree for period previous

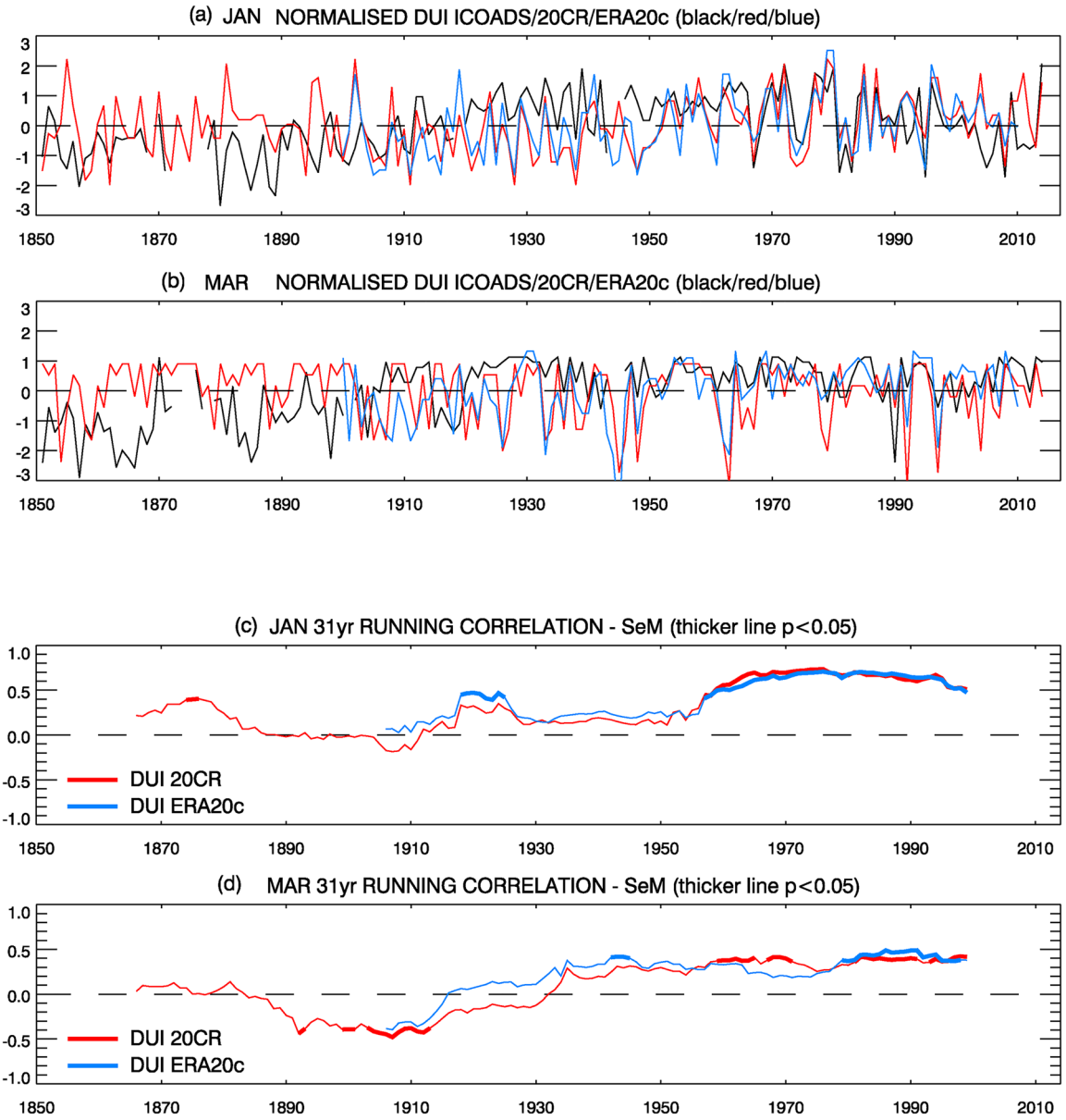

Figure 9. Comparison between the DUI computed from direct ICOADS wind direction observations (black line in [a] and [c] for January and March) and corresponding DUIs based on 20CR and ERA-20C reanalyzed wind (red and blue lines in [a] and [c]). Sliding correlations for a 31-years window between the ICOADS DUI and its 20CR and ERA-20C counterparts are shown in (c) and (d) (red and blue lines). Thicker lines indicate statistically significant correlations at $p < 0.05$.

Table 1
Pearson Correlation Coefficients Between DUI Computed From 20CR and ERA20C

	1900–1925	1926–1951	1952–1978	1979–2010
January	+0.72*	+0.71*	+0.81*	+0.88*
March	+0.32	+0.75*	+0.82*	+0.74*

Values marked with an asterisk are statistically significant at $p < 0.05$.

to the second half of the 20th century. This disagreement among 20th century reanalysis for periods of low data coverage has also been recently identified by Wohland et al. (2019) and this fact strongly suggests a significant impact of the assimilation scheme into the interannual variability of series derived from these datasets for periods and areas of sparse observation coverage.

We have also found this discrepancy between reanalyzes in the core of the upwelling season. Table 1 shows the Pearson correlation coefficients for the cases of January and March between the DUI computed from 20CR and ERA20C winds for the periods 1900–1925, 1926–1951, 1952–1978,

and 1979–2010. Although the last interval is longer as compared to the other, we selected it as representative of the post-satellite era. For the January case, correlations among the two reanalyzes are rather high and statistically significant along the entire study period, although the correlation increases for the periods corresponding to the second half of the 20th century. For the case of March, which is representative of the seasonal upwelling maxima, the correlation is noticeably lower and nonsignificant for the 1900–1925 period, as compared with the more recent ones.

4. Discussion

One of the most recurrent topics in the literature dealing with upwelling is the determination of its long-term trend. During the last three decades, this topic has been the subject of a vivid controversy. In the late 1980s, Dickson et al. (1988) first reported an increase in the northerly wind component over the eastern North Atlantic that would imply an upwelling intensification along the Iberian west coast. Later, Bakun generalized this result and first enunciated the "Upwelling Intensification Hypothesis" (Bakun, 1990). Under this scenario, greenhouse warming would diminish the nocturnal cooling and increase the diurnal warming. This would cause an amplified onshore-offshore atmospheric pressure gradient, intensifying the alongshore wind stress. In his original work (Bakun, 1990) Bakun presented observational evidence of a tendency to stronger upwelling in the northern portion of the CCUS, but for a relatively short period (1946–1985) and based on a network of wind observations that was sparse compared with today's standards. As new data have been made available, a lot of research has been undertaken to test this hypothesis, often with contradictory results.

At the CCUS, several authors have reported observational evidence supporting Bakun's hypothesis. For example, McGregor et al. (2007) found a significant decrease in SST reconstructed from Moroccan sediment cores in the northwest African margin over the 20th century consistent with increasing upwelling. From the examination of several reanalysis, and observed SSTs, Narayan et al. (2010) also reported a steady increase in the meridional wind stress for the period 1960–2001, but also found substantial differences among the results for the different datasets they considered, which were especially noticeable in the case of the CCUS. More recently, Cropper et al. (2014) performed a comprehensive analysis using multiple sources of data, finding strong evidence across several indices compatible with a summer upwelling increase in Northwest Africa above 20°N for the period 1981–2012. In contrast, Gomez-Gesteira et al. (2008) found a strong decrease in Canary upwelling intensity using a wind-derived Ekman transport index. Bonino et al. (2019) also found a negative upwelling trend there using passive tracers and connected it to the Atlantic Multi-decadal Oscillation. Barton et al. (2013) did not found any evidence of a coherent intensification of coastal winds using many databases and additionally, they documented a significant increase in SST values in several areas incompatible with an upwelling enhancement. Recent analyses of net primary production models applied to the CCUS present either significant decreases or nonsignificant changes, suggesting that no upwelling intensification is being experienced there, at least since the 1990s (Gómez-Letona et al., 2017). Modeling efforts have also provided ambiguous results, ranging from a consistent (although latitudinally dependent) upwelling increase under future climate change scenarios (Wang et al., 2015) to a lack of significant trend (Mote & Mantua, 2002) or even a change in the sign of the trend for different seasons (Sousa et al., 2017). Therefore, the question of whether the CCUS is increasing or not is far from being solved (Barton et al., 2013).

In this study, we try to shed light into this problem with a novel approach based on the use of the DUI, a wind circulation index constructed from in situ wind direction observations. The DUI reveals that the alongshore wind stress did not experience a long-term trend during the 20th century in our area of study. In this sense, our results do not support the Bakun hypothesis, at least in the 10°N–20°N section of the CCUS. Instead, we have found that the DUI has a noticeable interannual variability and superimposed to it, a large multidecadal variability. During the 19th century the DUI was persistently below its long-term average and the shift to present day values occurred in the five decades between 1870 and 1920, in a sequence of several decade-long fluctuations leading to an increase in the DUI average. This shift is independently observed in the 5 analyzed months. This is undoubtedly a striking result that would require independent confirmation. Unfortunately, other than the comparison with historical reanalysis that we have presented, we have not found another way to assess this change in the wind regime with independent data. Consequently, we have

scrutinized possible explanations for the presence of this shift considering the unusual characteristics of the data.

We have examined the possible impact on the DUI of the changes in data availability between 1825 and 2014 in the SeM box. The main increase in data availability is found between 1850 and 1880, while the main shift in the DUI is centered around 1900 and happened gradually up to 1920, not connected with sudden increases in data availability (see Figure 2c). We have also considered the possibility that the routes followed by the ships could have experienced abrupt changes along the decades. In this sense, it must be stressed that the DUI uncertainty have been explicitly evaluated by taking into account the observed variability in the geographical distribution of the observations (Figure 4). Even so, the observed DUI's shift is well above the magnitude of this uncertainty. Still, it is relevant to discuss the changes in the average location of the wind measurements. The direct analysis of the evolution of the average latitude and longitude of the wind observations (Figure 2d) does not reveal changes compatible with the observed shift. The average latitude of the observations remains essentially constant. In the case of the geographical longitude, a progressive eastward displacement of the routes is evident, and it is due to the increase of the routes circumnavigating Africa in relation to those followed by ships departing from Europe and aimed to South America, which ran further from the coast (see Figures 2b and 2d). However, the change occurred gradually and with the larger displacements concentrated on the second half of the 20th century, a period well after the observed shift in the DUI.

ICOADS contains observations from many different observing platforms ranging from early noninstrumental ship observations to more recent measurements from automatic systems such as moored buoys or surface drifters. In this sense, it could be possible that the changes in the nature of the observing platforms since the early 19th century could be introducing nonclimatic trends. To evaluate this possibility we performed an analysis of the relative importance of the observed platforms on the data used to build our DUI at the SeM box (figure not shown) and we did not find any evident change related to the shift. Most of the observations included in the DUI were taken aboard ships consistently along the study period. We also considered the possibility that the changes in the resolution in which the wind direction measurement was codified in ships could be introducing artificial biases. In this sense, during the 10th century a 16-point compass was quite frequently used to codify the wind direction (Wheeler, 2005), while a 32-point compass was more frequent in the 20th century. Moreover, as more precise instruments were incorporated to the meteorological equipment of ships along the 20th century, even finer resolutions are common. This progressive improvement in the resolution of the wind direction could result in an artificial trend in the DUI, as the numerical value of the DUI is directly dependent upon the relative number of wind direction observations between 315° and 45°. For example, a high-resolution measurement of wind direction of 47° would be discarded to compute the DUI, but most probably, this wind would have been codified as 45° in a 19th century logbook, and in this case, it would be incorporated in the DUI. Therefore, long-term trends in the DUI series could be affected by the improvements in the wind measurements. Under this assumption, it could be expected that during the early period of the DUI series the number of observations indicating pure 16-point directions such as 315° or 45° could be more frequent in relation with values slightly below 315 of above 45°, which would be more commonly found at the end of the series. Our analysis does not support this scenario. First because this would imply a progressive trend toward lower values of the DUI, which is contrary to the observed shift and second, because we explicitly computed the relative number of observations up to 10° lower that 315° and 10° greater than 45° and we found that there is no significant increment on the frequency of these cases along the study period.

Apart from the previous technical issues, we were also concerned with the fact that we define an unique index for an area covering the latitudes north and south of the 14°N parallel, the latitude that marks a change in the shelf morphology with a significant effect on the relative importance of the Ekman transport and the Ekman pumping. The former, predominant north of 14°N is mainly driven by the alongshore wind and is the one for which the DUI has been calibrated. The latter is more related to the wind stress curl (Jacox & Edwards, 2012). At the coarse spatial resolution necessary to define directional indices such as the DUI it is not possible to separate these effects (Castelao & Barth, 2006; Pickett & Paduan, 2003). Notwithstanding, it is usually considered that for a large-scale quantification of the upwelling intensity the indices relying on wind stress as our DUI integrate well enough the wind effect on the upwelling strength

(Cropper et al., 2014). We tested the sensitivity of the DUI to changes in the sampling area by computing an alternative DUI but only considering observations northward of 14°N. Apart from a greater uncertainty associated with the lower number of data available in the reduced domain and a small increase in the number of missing years, the downgraded DUI shows the same variability and, in particular, the same shift around the year 1900 (Figure not shown). A measurement of the similarities between the degraded and the complete DUI is given by the Pearson correlation coefficients between both versions of the DUI that results in $r = +0.91$ (January), $r = +0.91$ (February), $r = +0.90$ (March), $r = +0.88$ (April), and $r = +0.92$ (May) ($p < 0.01$ in all cases).

Finally, we compared our DUI based uniquely on direct wind observations (ICOADS DUI) with analogous indices computed from the 20CR and ERA-20C reanalysis. The ICOADS DUI has a quite good correlation with reanalysis-derived indices after the 1950s, especially with the 20CR reanalysis. On the contrary, for previous years, the correlation decreases, becoming even negative for some periods. Interestingly, for the first three decades of the 20th century, both reanalyzes also evidence relevant disagreements between them when estimating the persistence of the alongshore winds at the SeM. This disagreement could be due to the different observational constraint, the particularities of the assimilation model or most probably to a mixture of both causes. In this scenario, the differences in the climatic signal contained in the reanalysis would be more evident for periods of low data coverage and/or more uncertain observations, as it is the case of the biases on the wind speed on ICOADS, which are explicitly incorporated on ERA20C but not in 20CR. This kind of discrepancies at the time of quantifying wind circulation indices using historical reanalysis has also been found by Vega et al. (2017) and, at the present time, limits our ability of estimating long term tendencies in wind speed derived indices based on historical reanalysis.

5. Summary and Main Results

As a result of the efforts in data abstraction done during the last decades (Allan, 2011; Freeman, Kent, et al., 2019), a large number of wind direction observations are available since the first half of the 19th century in large areas of the oceans. By using these data, and a collection specifically abstracted for this study, we have been able to develop the longest series currently available quantifying the alongshore wind stress in the coast of Senegal and Mauritania.

The DUI reveals that the persistence of the northward winds between 10°N and 20°N is significantly correlated with the alongshore wind stress at monthly scale. For the period 1982–2014, the changes in the DUI are associated with low SST off the African coasts. These SST anomalies are statistically significant in large areas and they are especially noticeable in March, the core of the upwelling season. Because of the monthly scale and the large sampling area imposed by the nature of our data, the DUI does not catch some aspects of the upwelling dynamics at the southern CCUS, especially those related to fine details of the SST patterns. However, from the presented results and our previous experience with directional indices (see Garcia-Herrera et al., 2018 and references therein) we are confident in the performance of the DUI at the the time of characterizing the large scale variability of the wind circulation during long periods at the SeM area.

Our results indicate that the frequency of the alongshore winds along the West coast of Africa between 10°N and 20°N present a significant variability at decadal timescale. Regarding the long-term trends, the DUI did not experience a significant increase during the 20th century. However, we have found evidence of a shift toward more frequent alongshore winds in this region occurring around 1900. Although currently we cannot offer independent confirmation of this result, we have not found any other reason in our data that could explain this shift apart from climate variability. In this case, this shift would imply that a significant change in the upwelling intensity at the southern end of the CCUS should have occurred around 1900.

Data Availability Statement

ERA-20C data are provided by the European Center for Medium-Range Weather Forecasts and are available at: https://www.ecmwf.int/en/forecasts/datasets/reanalysis-datasets/era-20c. Operational Sea Surface Temperature and Ice Analysis data are provided by the Copernicus Marine Service (identifier SST_GLO_SST_L4_NRT_OBSERVATIONS_010_001).

Acknowledgments
Esther González did intensive work at the UK National Archives abstracting logbooks. The research was funded by the Spanish Ministerio de Economía y Competitividad under grant CGL2015-72164-EXP (UPNAO). Support for the 20th Century Reanalysis Project version 3 data set is provided by the U.S. Department of Energy, Office of Science Biological and Environmental Research (BER), by the National Oceanic and Atmospheric Administration Climate Program Office, and by the NOAA Physical Sciences Laboratory. Funding for open access publishing: Universidad Pablo de Olavide/CBUA.

References

Allan, R., Brohan, P., Compo, G. P., Stone, R., Luterbacher, J., & Brönnimann, S. (2011). The International Atmospheric Circulation Reconstructions over the Earth (ACRE) Initiative. *Bulletin of the American Meteorological Society*, *92*(11), 1421–1425. https://doi.org/10.1175/2011bams3218.1

Arístegui, J., Barton, E. D., Álvarez-Salgado, X. A., Santos, A. M. P., Figueiras, F. G., Kifani, S., et al. (2009). Sub-regional ecosystem variability in the Canary Current upwelling. *Progress in Oceanography*, *83*(1–4), 33–48. https://doi.org/10.1016/j.pocean.2009.07.031

Bakun, A. (1990). Coastal ocean upwelling. *Science*, *247*(4939), 198–201. https://doi.org/10.1126/science.247.4939.198

Bakun, A., Field, D. B., Redondo-Rodriguez, A., & Weeks, S. J. (2010). Greenhouse gas, upwelling-favorable winds, and the future of coastal ocean upwelling ecosystems. *Global Change Biology*, *16*(4), 1213–1228. https://doi.org/10.1111/j.1365-2486.2009.02094.x

Barriopedro, D., Gallego, D., Alvarez-Castro, M. C., García-Herrera, R., Wheeler, D., Peña-Ortiz, C., & Barbosa, S. M. (2014). Witnessing North Atlantic westerlies variability from ships' logbooks (1685-2008). *Climate Dynamics*, *43*, 939–955. https://doi.org/10.1007/s00382-013-1957-8

Barton, E. D., Field, D. B., & Roy, C. (2013). Canary current upwelling: More or less? *Progress in Oceanography*, *116*, 167–178. https://doi.org/10.1016/j.pocean.2013.07.007

Benazzouz, A., Mordane, S., Orbi, A., Chagdali, M., Hilmi, K., Atillah, A., et al. (2014). An improved coastal upwelling index from sea surface temperature using satellite-based approach - The case of the Canary Current upwelling system. *Continental Shelf Research*, *81*, 38–54. https://doi.org/10.1016/j.csr.2014.03.012

Bonino, G., Di Lorenzo, E., Masina, S., & Iovino, D. (2019). Interannual to decadal variability within and across the major Eastern Boundary Upwelling Systems. *Scientific Reports*, *9*(1). https://doi.org/10.1038/s41598-019-56514-8

Bosilovich, M. G., Kennedy, J., Dee, D., Allan, R., & O'Neill, A. (2013). On the reprocessing and reanalysis of observations for climate. In *Climate science for serving society* (pp. 51–71). Springer Netherlands. https://doi.org/10.1007/978-94-007-6692-1_3

Brönnimann, S., Allan, R., Atkinson, C., Buizza, R., Bulygina, O., Dahlgren, P., et al. (2018). Observations for reanalyzes. *Bulletin of the American Meteorological Society*, *99*(9), 1851–1866. https://doi.org/10.1175/bams-d-17-0229.1

Capet, X., Estrade, P., Machu, E., Ndoye, S., Grelet, J., Lazar, A., et al. (2017). On the dynamics of the southern Senegal upwelling center: Observed variability from synoptic to superinertial scales. *Journal of Physical Oceanography*, *47*(1), 155–180. https://doi.org/10.1175/jpo-d-15-0247.1

Cardone, V. J., Greenwood, J. G., & Cane, M. A. (1990). On trends in historical marine wind data. *Journal of Climate*, *3*(1), 113–127. https://doi.org/10.1175/1520-0442(1990)003<0113:otihmw>2.0.co;2

Castelao, R. M., & Barth, J. A. (2006). Upwelling around Cabo Frio, Brazil: The importance of wind stress curl. *Geophysical Research Letters*, *33*(3). https://doi.org/10.1029/2005gl025182

Cleveland, W. S. (1979). Robust locally weighted regression and smoothing scatterplots. *Journal of the American Statistical Association*, *74*(368), 829–836. https://doi.org/10.1080/01621459.1979.10481038

Compo, G. P., Whitaker, J. S., Sardeshmukh, P. D., Matsui, N., Allan, R. J., Yin, X., et al. (2011). The twentieth century reanalysis project. *Quarterly Journal of the Royal Meteorological Society*, *137*(654), 1–28. https://doi.org/10.1002/qj.776

Cropper, T. E., Hanna, E., & Bigg, G. R. (2014). Spatial and temporal seasonal trends in coastal upwelling off Northwest Africa, 1981-2012. *Deep Sea Research Part I: Oceanographic Research Papers*, *86*, 94–111. https://doi.org/10.1016/j.dsr.2014.01.007

Dickson, R. R., Kelly, P. M., Colebrook, J. M., Wooster, W. S., & Cushing, D. H. (1988). North winds and production in the eastern North Atlantic. *Journal of Plankton Research*, *10*(1), 151–169. https://doi.org/10.1093/plankt/10.1.151

Freeman, E., Kent, E. C., Brohan, P., Cram, T., Gates, L., Huang, B., et al. (2019). The international comprehensive ocean-atmosphere data set - meeting users needs and future priorities. *Frontiers Marine Science*, *6*. https://doi.org/10.3389/fmars.2019.00435

Freeman, E., Woodruff, S. D., Worley, S. J., Lubker, S. J., Kent, E. C., Angel, W. E., et al. (2016). ICOADS Release 3.0: A major update to the historical marine climate record. *International Journal of Climatology*, *37*(5), 2211–2232. https://doi.org/10.1002/joc.4775

Gallego, D., Garcia-Herrera, R., Calvo, N., & Ribera, P. (2007). A new meteorological record for Cádiz (Spain) 1806-1852: Implications for climatic reconstructions. *Journal of Geophysical Research*, *112*(D12). https://doi.org/10.1029/2007jd008517

Gallego, D., García-Herrera, R., Peña-Ortiz, C., & Ribera, P. (2017). The steady enhancement of the Australian Summer Monsoon in the last 200 years. *Scientific Reports*, *7*(1). https://doi.org/10.1038/s41598-017-16414-1

Gallego, D., Ordóñez, P., Ribera, P., Peña-Ortiz, C., & García-Herrera, R. (2015). An instrumental index of the West African Monsoon back to the nineteenth century. *Quarterly Journal of the Royal Meteorological Society*, *141*(693), 3166–3176. https://doi.org/10.1002/qj.2601

García-Herrera, R., Barriopedro, D., Gallego, D., Mellado-Cano, J., Wheeler, D., & Wilkinson, C. (2018). Understanding weather and climate of the last 300 years from ships' logbooks. *Wiley Interdisciplinary Reviews: Climate Change*, *9*(6), e544. https://doi.org/10.1002/wcc.544

García-Herrera, R., Können, G. P., Wheeler, D. A., Prieto, M. R., Jones, P. D., & Koek, F. B. (2005). CLIWOC: A Climatological Database for the World's Oceans 1750-1854. *Climatic Change*, *73*(1–2), 1–12. https://doi.org/10.1007/s10584-005-6952-6

Gómez-Gesteira, M., de Castro, M., Álvarez, I., Lorenzo, M. N., Gesteira, J. L. G., & Crespo, A. J. C. (2008). Spatio-temporal Upwelling Trends along the Canary Upwelling System (1967-2006). *Annals of the New York Academy of Sciences*, *1146*(1), 320–337. https://doi.org/10.1196/annals.1446.004

Gómez-Letona, M., Ramos, A. G., Coca, J., & Arístegui, J. (2017). Trends in primary production in the canary current upwelling system-a regional perspective comparing remote sensing models. *Frontiers Marine Science*, *4*. https://doi.org/10.3389/fmars.2017.00370

Good, S., Fiedler, E., Mao, C., Martin, M. J., Maycock, A., Reid, R., et al. (2020). The Current Configuration of the OSTIA system for operational production of foundation sea surface temperature and ice concentration analyses. *Remote Sensing*, *12*(4), 720. https://doi.org/10.3390/rs12040720

Haywood, J. M., Jones, A., Bellouin, N., & Stephenson, D. (2013). Asymmetric forcing from stratospheric aerosols impacts Sahelian rainfall. *Nature Climate Change*, *3*(7), 660–665. https://doi.org/10.1038/nclimate1857

Hersbach, H., Brönnimann, S., Haimberger, L., Mayer, M., Villiger, L., Comeaux, J., et al. (2017). The potential value of early (1939-1967) upper-air data in atmospheric climate reanalysis. *Quarterly Journal of the Royal Meteorological Society*, *143*(704), 1197–1210. https://doi.org/10.1002/qj.3040

Jackson, A., Jonkers, A. R. T., & Walker, M. R. (2000). Four centuries of geomagnetic secular variation from historical records. *Philosophical Transactions of the Royal Society of London, Series A: Mathematical, Physical and Engineering Sciences*, *358*(1768), 957–990. https://doi.org/10.1098/rsta.2000.0569

Jacox, M. G., & Edwards, C. A. (2012). Upwelling source depth in the presence of nearshore wind stress curl. *Journal of Geophysical Research*, *117*. https://doi.org/10.1029/2011jc007856

Jones, P. D., & Salmon, M. (2005). Preliminary reconstructions of the north Atlantic oscillation and the southern oscillation index from measures of wind strength and direction taken during the Cliwoc period. *Climatic Change*, *73*(1–2), 131–154. https://doi.org/10.1007/s10584-005-6948-2

Kalnay, E., Kanamitsu, M., Kistler, R., Collins, W., Deaven, D., Gandin, L., et al. (1996). The NCEP/NCAR 40-year reanalysis project. *Bulletin of the American Meteorological Society*, *77*(3), 437–471. https://doi.org/10.1175/1520-0477(1996)077<0437:tnyrp>2.0.co;2

Kanamitsu, M., Ebisuzaki, W., Woollen, J., Yang, S.-K., Hnilo, J. J., Fiorino, M., & Potter, G. L. (2002). NCEP-DOE AMIP-II Reanalysis (R-2). *Bulletin of the American Meteorological Society*, *83*(11), 1631–1643. https://doi.org/10.1175/bams-83-11-1631

McGregor, H. V., Dima, M., Fischer, H. W., & Mulitza, S. (2007). Rapid 20th-century increase in coastal upwelling off northwest Africa. *Science*, *315*(5812), 637–639. https://doi.org/10.1126/science.1134839

Mellado-Cano, J., Barriopedro, D., García-Herrera, R., & Trigo, R. M. (2020). New observational insights into the atmospheric circulation over the Euro-Atlantic sector since 1685. *Climate Dynamics*, *54*(1–2), 823–841. https://doi.org/10.1007/s00382-019-05029-z

Mellado-Cano, J., Barriopedro, D., García-Herrera, R., Trigo, R. M., & Hernández, A. (2019). Examining the North Atlantic Oscillation, East Atlantic Pattern, and Jet Variability since 1685. *Journal of Climate*, *32*(19), 6285–6298. https://doi.org/10.1175/jcli-d-19-0135.1

Mote, P. W., & Mantua, N. J. (2002). Coastal upwelling in a warmer future. *Geophysical Research Letters*, *29*(23), 53–61. https://doi.org/10.1029/2002gl016086

Narayan, N., Paul, A., Mulitza, S., & Schulz, M. (2010). Trends in coastal upwelling intensity during the late 20th century. *Ocean Science*, *6*(3), 815–823. https://doi.org/10.5194/os-6-815-2010

Ndoye, S., Capet, X., Estrade, P., Sow, B., Dagorne, D., Lazar, A., et al. (2014). SST patterns and dynamics of the southern Senegal-Gambia upwelling center. *Journal Geophysics Research: Oceans*, *119*(12), 8315–8335. https://doi.org/10.1002/2014jc010242

Ordoñez, P., Gallego, D., Ribera, P., Peña-Ortiz, C., & García-Herrera, R. (2016). Tracking the Indian Summer Monsoon Onset Back to the Preinstrument Period. *Journal of Climate*, *29*(22), 8115–8127. https://doi.org/10.1175/jcli-d-15-0788.1

Pickett, M. H., & Paduan, J. D. (2003). Ekman transport and pumping in the California Current based on the U.S. Navy's high-resolution atmospheric model (COAMPS). *Journal of Geophysical Research*, *108*(C10). https://doi.org/10.1029/2003jc001902

Poli, P., Hersbach, H., Dee, D. P., Berrisford, P., Simmons, A. J., Vitart, F., et al. (2016). ERA-20C: An atmospheric reanalysis of the twentieth century. *Journal of Climate*, *29*(11), 4083–4097. https://doi.org/10.1175/jcli-d-15-0556.1

Ramage, C. S. (1987). Secular change in reported surface wind speeds over the ocean. *Journal of Climate and Applied Meteorology*, *26*(4), 525–528. https://doi.org/10.1175/1520-0450(1987)026<0525:scirsw>2.0.co;2

Santos, F., deCastro, M., Gómez-Gesteira, M., & Álvarez, I. (2012). Differences in coastal and oceanic SST warming rates along the Canary upwelling ecosystem from 1982 to 2010. *Continental Shelf Research*, *47*, 1–6. https://doi.org/10.1016/j.csr.2012.07.023

Slivinski, L. C. (2018). Historical reanalysis: what, how, and why? *Journal of Advances in Modeling Earth Systems*, *10*(8), 1736–1739. https://doi.org/10.1029/2018ms001434

Sousa, M. C., Alvarez, I., deCastro, M., Gomez-Gesteira, M., & Dias, J. M. (2017). Seasonality of coastal upwelling trends under future warming scenarios along the southern limit of the canary upwelling system. *Progress in Oceanography*, *153*, 16–23. https://doi.org/10.1016/j.pocean.2017.04.002

Sydeman, W. J., García-Reyes, M., Schoeman, D. S., Rykaczewski, R. R., Thompson, S. A., Black, B. A., & Bograd, S. J. (2014). Climate change and wind intensification in coastal upwelling ecosystems. *Science*, *345*(6192), 77–80. https://doi.org/10.1126/science.1251635

Sylla, A., Mignot, J., Capet, X., & Gaye, A. T. (2019). Weakening of the Senegalo-Mauritanian upwelling system under climate change. *Climate Dynamics*, *53*(7–8), 4447–4473. https://doi.org/10.1007/s00382-019-04797-y

Thomas, B. R., Kent, E. C., Swail, V. R., & Berry, D. I. (2008). Trends in ship wind speeds adjusted for observation method and height. *International Journal of Climatology*, *28*(6), 747–763. https://doi.org/10.1002/joc.1570

Uppala, S. M., KÅllberg, P. W., Simmons, A. J., Andrae, U., Bechtold, V. D. C., Fiorino, M., et al. (2005). The ERA-40 re-analysis. *Quarterly Journal of the Royal Meteorological Society*, *131*(612), 2961–3012. https://doi.org/10.1256/qj.04.176

Vega, I., Gallego, D., Ribera, P., de Paula Gómez-Delgado, F., García-Herrera, R., & Peña-Ortiz, C. (2017). Reconstructing the Western North Pacific Summer Monsoon since the Late Nineteenth Century. *Journal of Climate*, *31*(1), 355–368. https://doi.org/10.1175/jcli-d-17-0336.1

Wang, D., Gouhier, T. C., Menge, B. A., & Ganguly, A. R. (2015). Intensification and spatial homogenization of coastal upwelling under climate change. *Nature*, *518*(7539), 390–394. https://doi.org/10.1038/nature14235

Wheeler, D. (2005). An examination of the accuracy and consistency of ships' logbook weather observations and records. *Climatic Change*, *73*(1–2), 97–116. https://doi.org/10.1007/s10584-005-6950-8

Wheeler, D., & García-Herrera, R. (2008). Ships' logbooks in climatological research. *Annals of the New York Academy of Sciences*, *1146*(1), 1–15. https://doi.org/10.1196/annals.1446.006

Wheeler, D., Garcia-Herrera, R., Wilkinson, C. W., & Ward, C. (2009). Atmospheric circulation and storminess derived from Royal Navy logbooks: 1685 to 1750. *Climatic Change*, *101*(1–2), 257–280. https://doi.org/10.1007/s10584-009-9732-x

Wilkinson, C., Woodruff, S. D., Brohan, P., Claesson, S., Freeman, E., Koek, F., et al. (2011). Recovery of logbooks and international marine data: The RECLAIM project. *International Journal of Climatology*, *31*(7), 968–979. https://doi.org/10.1002/joc.2102

Wohland, J., Omrani, N., Witthaut, D., & Keenlyside, N. S. (2019). Inconsistent wind speed trends in current twentieth century reanalyzes. *Journal of Geophysical Research: Atmospheres*, *124*(4), 1931–1940. https://doi.org/10.1029/2018jd030083

Woodruff, S. D., Worley, S. J., Lubker, S. J., Ji, Z., Eric Freeman, J., Berry, D. I., et al. (2010). ICOADS Release 2.5: Extensions and enhancements to the surface marine meteorological archive. *International Journal of Climatology*, *31*(7), 951–967. https://doi.org/10.1002/joc.2103